Exchange anisotropy pinning of a standing spin-wave mode

R. Magaraggia, K. Kennewell, M. Kostylev, and R. L. Stamps
School of Physics, University of Western Australia, 35 Stirling Highway, Crawley, Western Australia 6009, Australia

M. Ali, D. Greig, B. J. Hickey, and C. H. Marrows
School of Physics and Astronomy, E. C. Stoner Laboratory, University of Leeds, Leeds LS2 9JT, United Kingdom
(Received 22 July 2010; published 8 February 2011)

Standing spin waves in a thin film are used as sensitive probes of interface pinning induced by an antiferromagnet through exchange anisotropy. Using coplanar waveguide ferromagnetic resonance, pinning of the lowest energy spin-wave thickness mode in $Ni_{80}Fe_{20}/Ir_{25}Mn_{75}$ exchange-biased bilayers was studied for a range of $Ir_{25}Mn_{75}$ thicknesses. We show that pinning of the standing mode can be used to amplify, relative to the fundamental resonance, frequency shifts associated with exchange bias. The shifts provide a unique "fingerprint" of the exchange bias and can be interpreted in terms of an effective ferromagnetic film thickness and ferromagnet-antiferromagnet interface anisotropy. Thermal effects are studied for ultrathin antiferromagnetic $Ir_{25}Mn_{75}$ thicknesses, and the onset of bias is correlated with changes in the pinning fields. The pinning strength magnitude is found to grow with cooling of the sample, while the effective ferromagnetic film thickness simultaneously decreases. These results suggest that exchange bias involves some deformation of magnetic order in the interface region.

DOI: 10.1103/PhysRevB.83.054405 PACS number(s): 75.30.Gw, 75.70.Cn, 76.50.+g

I. INTRODUCTION

Exchange bias is an effect which has consequences for the bulk of a ferromagnet as exhibited by hysteresis loop offset. However, its bulk effects arise from coupling processes across a ferromagnetic-antiferromagnetic interface.[1,2] Directly probing these types of buried interfaces to gain information on coupling is quite challenging. Ferromagnetic resonance (FMR) is a powerful tool for studying magnetic parameters in ferromagnetic structures through frequency shifts of the fundamental resonance mode. It is possible to also use FMR to detect standing spin waves which provide, at least in principle, information about surfaces and buried interfaces.[3–5] In this paper standing spin waves (also referred to as "thickness modes") are used to probe interface properties due to exchange anisotropies in exchange-biased bilayers. We show that a useful measure for characterizing exchange bias can be obtained from these modes, and this measure can provide unique information about magnetic ordering in the interface region.

Nearly all studies of ferromagnetic resonance and spin waves in exchange-biased structures have, to date, made use exclusively of the fundamental resonance or zone center spin waves.[4,6,7] The frequencies of these excitations are governed primarily by local magnetocrystalline and shape anisotropies, magnetization, and the applied field. The resonance conditions for a ferromagnetic thin film with no intrinsic anisotropies, and magnetized in plane, is given by[8]

$$\left(\frac{\omega}{\gamma}\right)^2 = \left[H_f(\theta) + Dk_y^2(\theta)\right]\left[H_f(\theta) + \mu_0 M_s + Dk_y^2(\theta)\right]. \tag{1}$$

The spin-wave frequency is ω, γ is the gyromagnetic ratio, M_s is the saturation magnetization, H_f is the field applied to cause resonance, and θ is the direction of the applied field relative to the cooling-field direction. A fixed spin-wave frequency is assumed and θ is varied, so that H_f becomes the experimentally measured quantity. The wave-vector component in the direction normal to the film plane is k_y. The $\mu_0 M_s$ term originates from dynamic demagnetization fields in thin-film geometry, and $D = \frac{2A}{M_s}$ is the exchange coupling strength. In traditional treatments of FMR as applied to exchange bias the fundamental FMR mode corresponds to $k = 0$. Effective fields originating at the interface with the antiferromagnet are then, as far as the FMR response is concerned, averaged over the ferromagnetic film thickness and are seen as an effective anisotropy field. In a resonance experiment using a fixed frequency, these effective fields appear in the measured value of H_f, the applied field for which resonant absorption is observed. It is important to note that the frequency shifts of the FMR associated with exchange bias do not contain direct information about the interface region per se. Questions concerning the penetration depth of the interface fields, or asymmetries associated with different boundaries, can only be addressed indirectly by varying film thicknesses within a series of samples. A disadvantage of this approach is that samples can vary substantially, even within the same series due to details of growth processes.[1,9]

The FMR mode averages local interface fields laterally because it is a long-wavelength excitation, though in reality it does experience deformation due to the interfacial pinning. In some cases, short-wavelength spin waves can be observed with conventional resonance techniques as standing wave thickness modes confined by film geometry. It is access to these modes which allows a measure of interface pinning. Recently, we have shown theoretically and experimentally that broadband FMR driving techniques that make use of stripline or coplanar waveguides can couple effectively to thickness modes in metallic multilayers.[10,11] These thickness modes have some discrete wave vector $k_y(\theta)$, and therefore they involve contributions from exchange. Hereafter these modes are referred to as "FEX modes." These will each have different allowed wave vectors confined in the y direction, as determined by surface pinning. As such, the frequencies of the FEX modes include contributions from exchange and are sensitive to

surfaces and interfaces. The lower symmetry at film boundaries can give rise to local anisotropy fields, and interfaces between different magnetic layers can support exchange coupling. In these cases, spin-wave oscillations may be pinned at one or more boundaries of a ferromagnetic film. Pinning of this type is accompanied by contributions through exchange energies and can result in substantial frequency shifts.[12]

A simple means of analyzing frequencies obtained for thickness modes was suggested long ago by Rado and Weertman.[13,14] In this approach, surface anisotropies are assumed, which then dictate the boundary conditions for FEX modes in thin-film geometries. It should be noted that the FMR mode will also be affected and given a nonzero wave vector resulting from surface pinning. If we associate a surface energy[15] of the following form with the exchange-biased interface:

$$E_{\mathrm{SA}} = p \cdot M_s, \tag{2}$$

we can then calculate allowed spin-wave wave vectors as a result of pinning. In this equation M_s is the saturation magnetization and p is the pinning parameter, which acts parallel to the applied field. As demonstrated in Ref. 13, if one starts with the Landau-Lifshitz equation and integrates over an infinitesimal volume region across the interface, the following is obtained:

$$\left(\frac{2A}{M_s}\right)\boldsymbol{M} \times \frac{\partial \boldsymbol{M}}{\partial n} + \boldsymbol{T}_{\mathrm{surf}} = 0. \tag{3}$$

Here **M** represents the total magnetization, n is the direction normal to the interface, and $\boldsymbol{T}_{\mathrm{surf}}$ is the interface torque. Using Eq. (2), we have

$$\boldsymbol{T}_{\mathrm{surf}} = -\boldsymbol{M} \times \nabla_M E_{\mathrm{SA}} = -\boldsymbol{M} \times p. \tag{4}$$

We approximate the exchange-biased interface by supposing the pinning to come entirely from one of the boundaries, hence introducing an asymmetry into the model. After solving Eq. (3) in combination with Eq. (4), the relationship between these surface anisotropies and k_y for H_f applied at an angle θ to the easy axis is

$$p(\theta) = \left(\frac{2A}{M_s}\right)\left[\frac{-k_y(\theta)}{\cot(k_y(\theta)t_{\mathrm{eff}})}\right]. \tag{5}$$

It is important to note that t_{eff} is the magnetic thickness of the ferromagnet, as opposed to the structural thickness (which may be different).[16,17] This difference may be caused by deviations away from uniform ferromagnetic order near the interface due to local pinning fields.

The remainder of the paper is organized as follows. First, preparation of, and magnetization measurements from, exchange-biased $Ni_{80}Fi_{20}/Ir_{25}Mn_{75}$ are discussed. Next we present results from coplanar FMR studies of the fundamental and first thickness modes for these structures, and we discuss their interpretation in terms of the pinning parameter p and effective thickness t_{eff}.

II. SAMPLE PREPARATION AND CHARACTERIZATION

Magnetic bilayer specimens consisting of Ta(50Å)/$Ni_{80}Fe_{20}$(605Å)/$Ir_{25}Mn_{75}$(t_{AF}Å)/Ta(50Å) were sequentially deposited onto Si(001) substrates by dc magnetron sputtering at an argon working pressure of 2.5 mTorr to minimize growth variations. A nanometer layer of native oxide on the silicon surface created conditions for polycrystalline growth. Typical deposition rates were 2–2.5 Å s^{-1}, which were determined by measuring the thickness of calibration films by low-angle x-ray reflectometry. The base pressure prior to the deposition was of the order of 1×10^{-8} Torr and the samples were deposited at ambient temperature. An in-plane forming field of 200 Oe was applied during the growth to induce a macroscopic uniaxial anisotropy in the NiFe (Py) layer in a defined direction. The thickness of the IrMn layer, t_{AF}, for this study was varied from 0 to 60 Å, which is also the region where the onset of biasing appears at room temperature for such systems.[18] The samples were cut into 10×10 mm squares.

Film thickness was accurately characterized with a Siemens two-circle diffractometer, to within ±6 Å. Additional measurements on bare permalloy samples show that the surface roughness is approximately 3 Å. In-plane and out-of-plane FMR magnetometry was used to extract $\mu_0 M_s$, which could consistently be used in further FMR data analysis. In-plane FMR magnetometry along the easy axis of a Py sample with no IrMn revealed a saturation magnetization $\mu_0 M_s$ of 0.80 ± 0.05 T, a gyromagnetic ratio γ of 2.8×10^{10} Hz T^{-1}, and in-plane bulk anisotropy fields of 0.0002 ± 0.0005 T. Further magnetometry was performed using the magneto-optical Kerr effect (MOKE). A 635-nm diode laser, rated at 5 mW, was used to illuminate the sample. A differential amplifier was used to analyze polarization rotation. Example results are shown in Fig. 1.

As demonstrated in Fig. 1, the samples saturate magnetically below −20 Oe. The loops are nonsymmetric about a nonzero field with a small coercivity, and they compare well with what has been found in similar studies.[7,19] The bias field as measured with FMR is defined as $H_{\mathrm{EB}} = (H_{f^+} - H_{f^-})/2$,

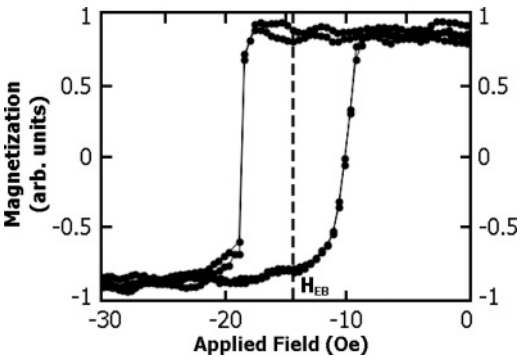

FIG. 1. A sample of data taken with a MOKE magnetometry setup focused onto the NiFe(60.5 nm)/IrMn(6 nm) sample. The vertical axis uses arbitrary units and represents the average magnetization over the laser spot focused onto the sample. The horizontal axis displays the field applied across the sample in units of oersteds. The MOKE data were gathered via a repetitive field sweeping technique with averaging over thousands of cycles. For data shown in this picture, averaging was done over two field sweeps, which resulted in a double hysteresis loop, with the difference between the two loops determined by the level of noise in the system. Also the exchange-bias shifting of the loop is shown by the dotted line and denoted by H_{EB}.

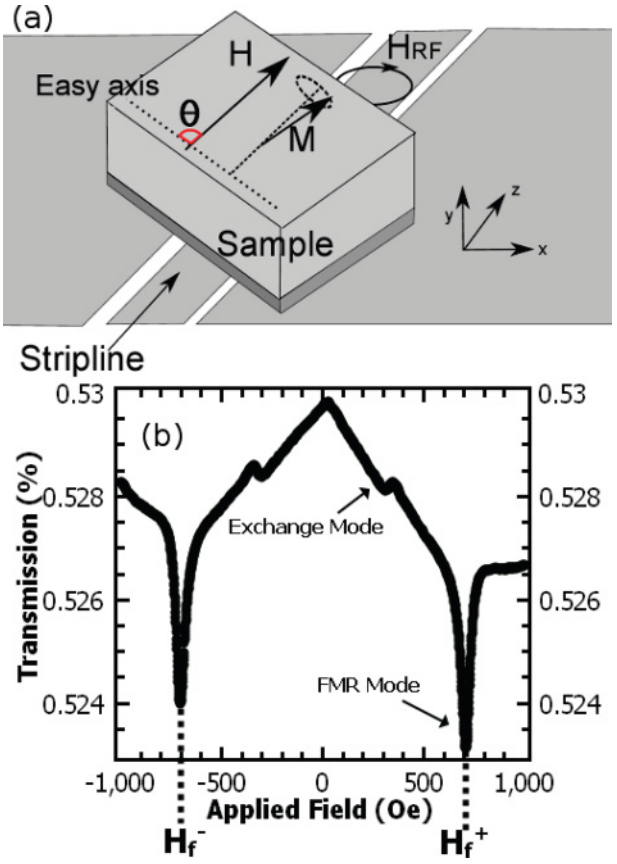

FIG. 2. (Color online) (a) The experimental geometry, with the sample placed on top of the coplanar stripline. H refers to the applied field direction at some angle θ, M refers to the magnetization direction, and H_{RF} refers to the microwave rf field generated by the waveguide. The sample is rotated in place in order to change the direction of H with respect to the sample's easy axis. (b) Microwave transmission as a function of static applied field for the 0-nm IrMn sample. The values $H_f\pm$ correspond to applied resonant fields in antiparallel directions for $+$ and $-$, respectively. Seen are microwave absorptions which correspond to the fundamental mode (FMR) and the first exchange mode (FEX). The microwave excitation frequency ω used was 7 GHz.

shown in Fig. 2, where H_{f^+} corresponds to $H_f(0)$ in Eq. (1), and H_{f^-} corresponds to $H_f(\pi)$.

III. RESONANCE MEASUREMENTS AND INTERPRETATION

A 20-GHz vector network analyzer (VNA) was used to excite and detect FMR and FEX modes of the samples. The coplanar stripline (1.6 mm wide), which is coupled to 50-Ω coaxial cables, excites the sample with microwaves in the 2–9 GHz regime. Excitation of traveling spin-wave modes due to finite stripline width is estimated to have a minimal effect on measured resonance fields compared to other experimental uncertainties.[20,21] Example results are shown in Fig. 2. We choose a particular excitation frequency ω and sweep the applied magnetic field H (usually between 0 and 600 Oe) in a particular direction until microwave power is absorbed strongly by the sample, indicating a standing spin wave is on resonance. This procedure is repeated for the samples' easy axis aligned along different directions with respect to the applied field, denoted by θ. A field sweep was chosen rather then a frequency sweep, as a field sweep avoids the problems of variable microwave frequency attenuation in the waveguides with varying ω and shows the magnetic response of the sample as opposed to both magnetic and electric response.

An example of FMR and FEX resonances, at a driving frequency of 7 GHz, is shown in Fig. 2(b). A number of factors determine the observed amplitudes of FMR and FEX modes in coplanar geometries,[11,22–25] in particular a combination of surface pinning and eddy-current-induced inhomogeneity in the driving microwave field. The FEX absorption amplitude is approximately 1/23 that of the FMR mode as measured at 7 GHz. The linewidths of the modes at 7 GHz are $\Delta f_{FMR} = 49$ Oe and $\Delta f_{FEX} = 25$ Oe, respectively. It should be noted that the FMR mode has a Lorentzian-like absorption shape, but the FEX mode does not, so the linewidths may not be directly comparable. The difference between absorption shapes seems to lie in an electrical phase shifting between the rf signal from the FMR mode and the rf signal from the FEX mode. This difference is seen for VNA microwave scattering parameters both in the transmission |S21| data in Fig. 2(b) and in the Re(S21) data. Possible causes include an additional phase shift due to the broad magnetic background of the coplanar waveguide, or something intrinsic in how the two modes behave when excited by the coplanar setup. The actual reason for this phase shift is unknown to the authors.

The bias determined from FMR and FEX are shown in comparison to the bias determined from MOKE data in Fig. 3. Unidirectional exchange anisotropies are present at room temperature only for a certain critical thickness >2.5 nm of IrMn as shown in Fig. 3.

For thicknesses above this value, the MOKE and FEX results indicate a nearly monotonic behavior of the bias with respect to IrMn thickness beginning at 4 nm. Most significantly, the pinning field is unidirectional. This is fully consistent with exchange bias as an interface effect. The bias acts as an effective volume unidirectional anisotropy when averaged by the FMR mode, and it appears as a superposition

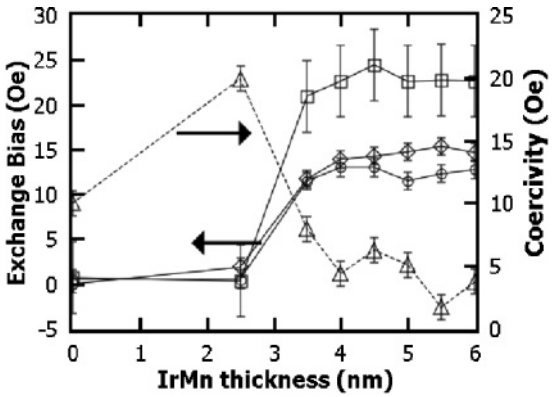

FIG. 3. The exchange bias as measured from the FMR mode (empty circles, solid line), MOKE (empty diamonds, solid line), and FEX mode (empty squares, solid line), as a function of IrMn film thickness. The NiFe layer thickness is always 60.5 nm. For comparison the coercivity as measured with MOKE is shown (empty triangles, dashed line).

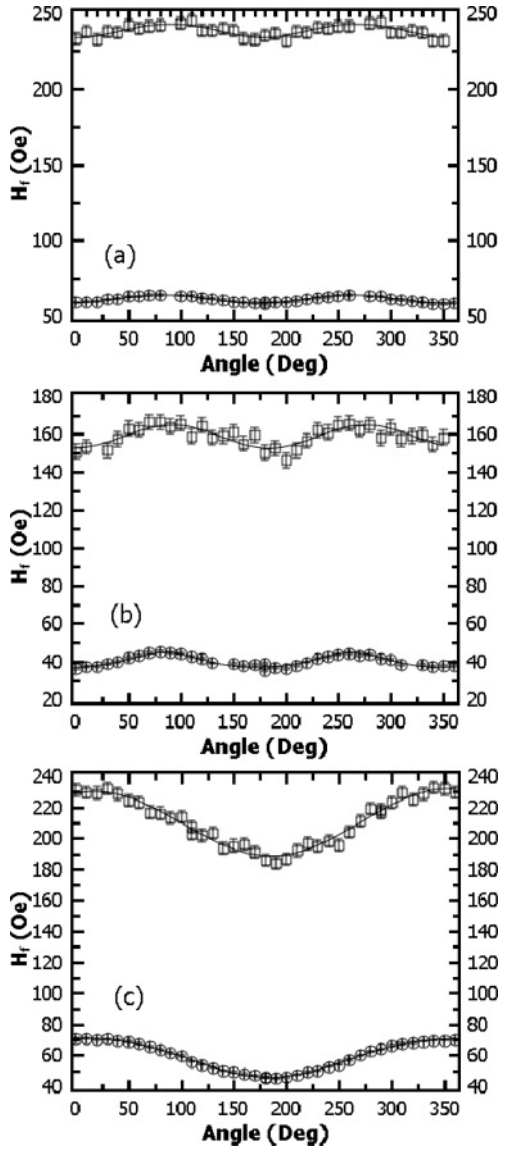

FIG. 4. Resonant fields H_f for the FMR (empty circles) and FEX (empty squares) standing spin-wave modes at different applied field angles with respect to the easy axis (θ). The solid lines show fits to the data using $\cos(\theta)$ and $\cos(2\theta)$ components. Presented are the resonance data for different IrMn thickness capping layers: (a) IrMn = 0 nm, (b) IrMn = 2.5 nm, and (c) IrMn = 6 nm.

with other volume anisotropies. This superposition can be seen most clearly by measuring bias at different orientations of the applied field relative to the bias field direction. Example results for the 2.5- and 6-nm-thick IrMn samples are shown in Fig. 4. Results for FMR and FEX peaks are shown as a function of angle, demonstrating that both modes contain equal contributions from a uniaxial anisotropy, whereas the modes are affected differently by the exchange bias.

The results shown in Fig. 4 illustrate the magnitude of exchange bias as measured by the FMR and FEX modes. The difference in magnitude can be understood through pinning effects on the frequency of the FEX modes. The FEX modes contain greater exchange energy than the FMR modes because of their shorter wavelengths, and pinning acts to effectively change the wavelength of an FEX mode. In this way, pinning by exchange bias amplifies the exchange anisotropy by affecting directly the exchange energy contribution to an FEX mode. This is demonstrated explicitly in Eq. (1), where the exchange-related effective anisotropy field Dk_y^2 scales as the square of the wave number k_y. Therefore one should expect different strengths of effective anisotropy from the FMR and FEX modes. Indeed, such differences are seen in Fig. 4 for these two modes, confirming the interface origins of the anisotropy fields in this exchange-biased system.

Pinning factors p are calculated by using Eq. (1) to find the spin-wave wave number k_y from experimental data, then Eq. (5) is used to extract the corresponding p. Variation in p as a function of IrMn thicknesses is shown in Fig. 5 for data taken at room temperature. Interface anisotropy calculated for the applied field along $\theta = 0^\circ$ is denoted $p(\theta = 0^\circ)$ and represents the situation where the applied field is antiparallel to the bias field direction. Conversely, $p(\theta = 180^\circ)$ is the pinning calculated for the field applied along the bias direction $\theta = 180^\circ$. In these calculations, we have used material parameters determined experimentally as above. The exchange coupling strength $D = 1.3693 \times 10^{-17}$ J A^{-1} was chosen such that an effective thickness of 60.5 nm was extracted from the monolayer permalloy film. Error bars in Fig. 5 were estimated by incorporating experimental field uncertainties. We consider p as the more fundamental quantity than the exchange-bias field. Pinning will act with the same strength on both modes, but the wavelength of each mode will be distorted to a different degree. Importantly, in our fittings we have the condition that p should have the same value for all observed modes. We find

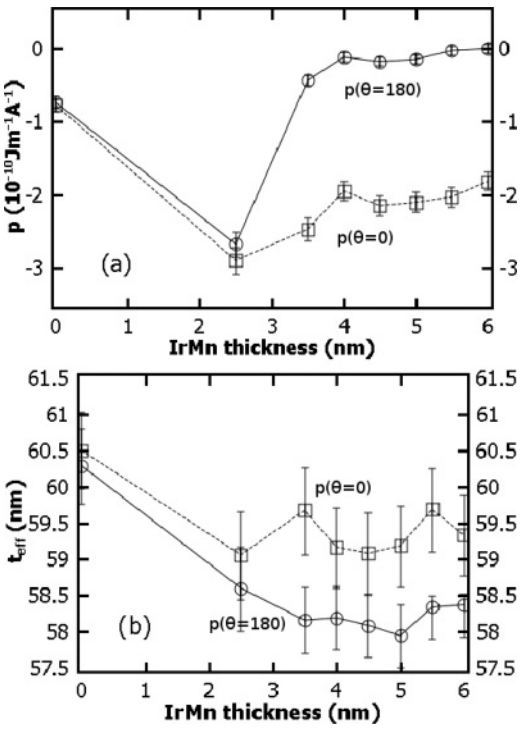

FIG. 5. (a) The calculated strengths of pinning $p(\theta = 180)$ along the bias direction (empty circles, solid line) and $p(\theta = 0)$ against the bias direction (empty squares, dashed line). (b) The corresponding effective magnetic thickness t_{eff} of the NiFe along the bias direction (empty circles, solid line) and against the bias direction (empty squares, dashed line).

that this condition cannot be satisfied unless some value is modified for one of the physical parameters in Eq. (5). The derivations of Eq. (5) and previous works[16,17] suggest that the suitable parameter is the thickness of the ferromagnetic layer. Therefore the second parameter extracted from the fits is the effective thickness of the ferromagnetic layer. As previously mentioned, the difference between t_{eff} and the structural thickness of the ferromagnet might be related to deviation from uniform ferromagnetic order close to the interface.

The dependence of p on IrMn thickness shows a curious peak for the 4-nm-thick film, but otherwise it is a nearly linear function of t_{AF} above 2.5 nm. In addition to an interface pinning, we also simultaneously extract an effective magnetic thickness t_{eff} from the data. The greatest change of t_{eff} with in-plane field direction appears for t_{AF} between 5 and 5.5 nm, a range in which the largest degree of exchange bias is observed with MOKE but not FMR.

Like p, the effective thickness varies as a function of applied field direction. The IrMn free permalloy layer [Fig. 6(a)] does not show any significant variation of t_{eff} with θ, with the implication that no significant micromagnetic configurational changes take place when aligning the magnetization along different anisotropy directions. This is in sharp contrast to the 6-nm IrMn film [Fig. 6(b)], which does display a roughly 1-nm thickness variation of t_{eff} over the angular range 0° to 180°.

An interpretation of effective magnetic film thickness is difficult as it does not allow identification of specific micromagnetic structures across the interface region. Nevertheless, it does not seem unreasonable that t provides some measure of the size over which magnetization in the interface region contributes to pinning, perhaps through local modification of the magnetic order.[17,26] In particular, polarized neutron scattering and x-ray techniques which have probed similar exchange-biased systems reveal that there do exist deviations of magnetic order around the interfaces of up to a few nanometers,[27] although without a detailed comparative study it is difficult to directly compare findings between the two.

Lastly, we discuss the measured dependence of bias and pinning on temperature for the 2.5-nm-thick IrMn bilayer. This layer was most interesting because it does not show significant bias at room temperature, but it does develop bias at lower temperatures. A summary of results is shown in Fig. 7. A linear increase in exchange bias below 240 K was found from the FMR mode data, and this has been reported previously in the literature.[28–30] A linear increase in the magnitude of the pinning parameters was found over the same temperature region, with different slopes for p measured parallel and antiparallel to the bias direction. The behavior of t_{eff} however reveals that it remains almost unaffected for most of the temperature range, and for the lowest temperatures it splits between the two applied field directions. The interfacial region involved in pinning is determined by the difference between

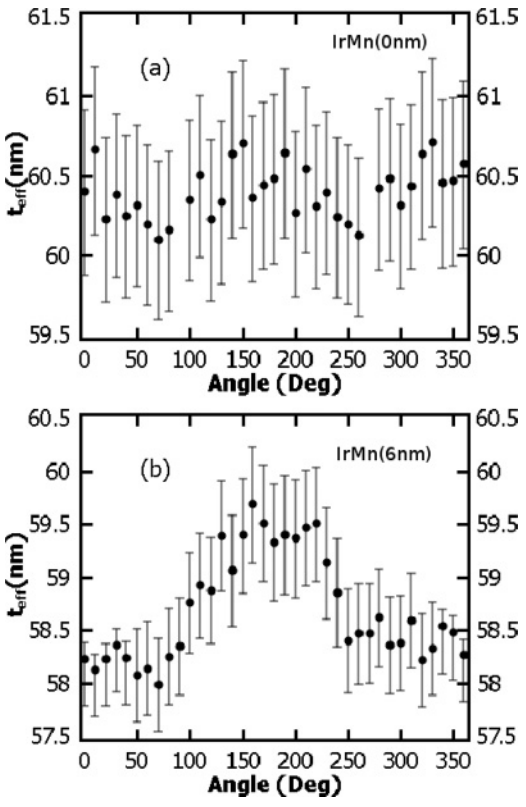

FIG. 6. The effective magnetic thickness of NiFe as a function of θ with respect to the easy axis for (a) a 0-nm IrMn film and (b) a 6-nm IrMn film.

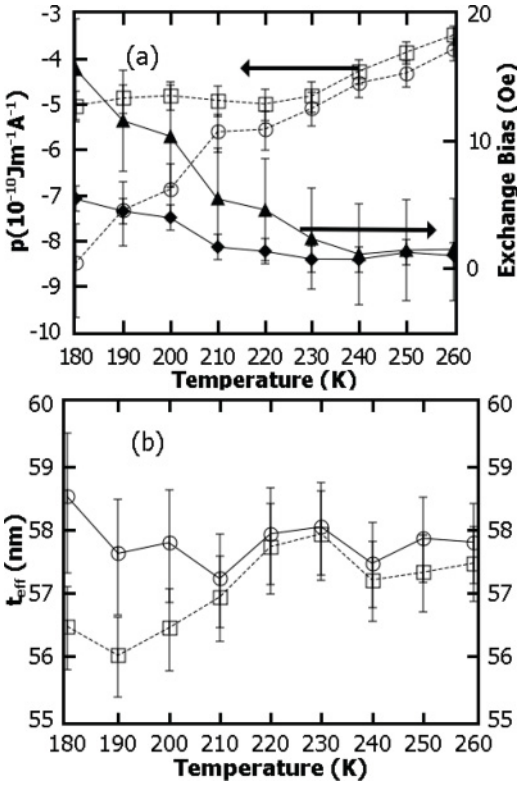

FIG. 7. (a) The calculated strengths of pinning $p(\theta = 180)$ along the bias direction (empty circles, dashed line) and $p(\theta = 0)$ against the bias direction (empty squares, dashed line) for the IrMn 2.5-nm film cooled to the temperature indicated on the horizontal axis, in a 40-Oe field. Also shown is the complementary information on the exchange-bias shift for the FMR mode (solid triangles, solid line) and FEX mode (solid diamonds, solid line). (b) The corresponding effective magnetic thickness t_{eff} of the NiFe along the bias direction (empty circles, solid line) and against the bias direction (empty squares, dashed line) for the same range of field-cooled temperatures.

values obtained from parallel and antiparallel orientations. This difference is about 2 nm, with large uncertainties.

IV. DISCUSSION AND CONCLUSIONS

In this paper we have presented results for resonant field shifts due to exchange bias in NiFe-IrMn bilayers. The unidirectional exchange anisotropy was determined from angular resolved resonance experiments. We observed field differences for the lowest order standing spin-wave mode that are twice the magnitude of the corresponding difference for the fundamental resonance. We showed that interpretation of these results can be made in terms of pinning effects due to an effective surface exchange anisotropy. The distortion each spin-wave mode experiences due to this pinning is not the same for every mode. Experimentally this results in different exchange anisotropies observed for FMR and FEX resonances. The assumption of an effective surface anisotropy is possible because resonances of IrMn are at much higher frequencies than those probed with our coplanar resonance technique, so that the NiFe spin waves are driving the IrMn far off resonance. Because of this mismatch in frequencies, the effective fields acting on the NiFe spins near the interface are governed by anisotropies induced through exchange coupling to the IrMn spins, and other dynamics in the antiferromagnet can be safely neglected.[12,31] One can understand the pinning simply as a unidirectional anisotropy whose magnitude varies as $\cos(\theta)$, where θ is the angle of the static field relative to the bias direction.

When calculating the wave vectors of the FMR and FEX modes, deviations from values expected assuming no pinning are found. Analyzing the data this way returns a pinning parameter that characterizes the strength of interface coupling and gives an effective magnetic thickness over which the NiFe film acts as a saturated ferromagnet. As the structural thickness of the NiFe films are well known, deviations from this value in t_{eff} may arise from the magnetization close to the interface. Thus one can also interpret the observed effective thickness as an exchange-bias effect that involves a deformation of the magnetization near the interface that reduces the magnetic thickness of the ferromagnet participating in the spin-wave resonance. Such a deformation might be possible through either pinning of ferromagnetic spins near the interface or formation of a twist on the ferromagnet side of the interface. We note that this interpretation is analogous to the effective boundary conditions derived by Guslienko and Slavin for dipolar contributions to resonance in stripes.[15]

The spin-wave probe technique is not the only magnetically sensitive interfacial probe technique. Other magnetic interface probing techniques, such as polarized neutron reflectivity and x-ray reflectivity, can be tuned to provide information about magnetization as a function of depth into an exchange-biased sample. X-ray reflectivity may also be tuned to be element specific, as shown in Ref. 27. While scattering techniques provide information about the spin configuration throughout the entire film, the spin-wave technique gives information about coupling strength across the ferromagnet to antiferromagnet along with a crude parameter to describe magnetization deformation effects.

We close with two final remarks. First, there exists a difference between exchange-bias measurements between FMR and MOKE of at most 30%. This is a well-known effect[32] and is due primarily to FMR being a perturbative measurement of local fields whereas MOKE measurements of hysteresis necessarily involve magnetization processes. Though there has not previously been an FEX to MOKE comparison, we note that FEX follows the same trend as the FMR data, but with different magnitude as both are perturbative measures of the exchange anisotropy. Second, possible effects associated with field cooling were also sought. As shown here, the 2.5-nm IrMn sample has a blocking temperature below room temperature and it does not experience significant exchange biasing until below 240 K.

ACKNOWLEDGMENTS

Support from the Australian Research Council under the Discovery and Australian Postgraduate Award programmes is acknowledged. Furthermore, support from the United Kingdom's Engineering and Physical Sciences Research Council is also acknowledged.

[1] J. Nogués and I. K. Schuller, J. Magn. Magn. Mater. **192**, 203 (1999).
[2] R. Stamps, J. Phys. D **33**, R247 (2000).
[3] W. Stoecklein, S. S. P. Parkin, and J. C. Scott, Phys. Rev. B **38**, 6847 (1988).
[4] R. D. McMichael, M. D. Stiles, P. J. Chen, and W. F. Egelhoff, Phys. Rev. B **58**, 8605 (1998).
[5] C. Kittel, Phys. Rev. **110**, 1295 (1958).
[6] B. K. Kuanr, S. Maat, S. Chandrashekariaih, V. Veerakumar, R. E. Camley, and Z. Celinski, J. Appl. Phys. **103**, 07C107 (2008).
[7] J. McCord, R. Mattheis, and D. Elefant, Phys. Rev. B **70**, 094420 (2004).
[8] C. Kittel, *Introduction to Solid State Physics*, 8th ed. (Wiley, New York, 2005).
[9] A. E. Berkowitz and K. Takano, J. Magn. Magn. Mater. **200**, 552 (1999).
[10] M. Kostylev, J. Appl. Phys. **106**, 043903 (2009).
[11] K. J. Kennewell, M. Kostylev, N. Ross, R. Magaraggia, R. L. Stamps, M. Ali, A. A. Stashkevich, D. Greig, and B. J. Hickey, J. Appl. Phys. **108** (2010).
[12] R. L. Stamps, R. E. Camley, and R. J. Hicken, Phys. Rev. B **54**, 4159 (1996).
[13] G. Rado and J. Weertman, J. Phys. Chem. Solids **11**, 315 (1959).
[14] P. Yen, T. S. Stakelon, and P. E. Wigen, Phys. Rev. B **19**, 4575 (1979).
[15] K. Y. Guslienko and A. N. Slavin, Phys. Rev. B **72**, 014463 (2005).
[16] S. Brück, G. Schütz, E. Goering, X. Ji, and K. M. Krishnan, Phys. Rev. Lett. **101**, 126402 (2008).
[17] S. Roy *et al.*, Phys. Rev. Lett. **95**, 047201 (2005).
[18] M. Ali, C. H. Marrows, and B. J. Hickey, Phys. Rev. B **67**, 172405 (2003).

[19]C. Leighton and I. K. Schuller, Phys. Rev. B **63**, 174419 (2001).
[20]G. Counil, J.-V. Kim, T. Devolder, C. Chappert, K. Shigeto, and Y. Otani, J. Appl. Phys. **95**, 5646 (2004).
[21]K. J. Kennewell, M. Kostylev, and R. L. Stamps, J. Appl. Phys. **101**, 09D107 (2007).
[22]W. S. Ament and G. T. Rado, Phys. Rev. **97**, 1558 (1955).
[23]R. D. McMichael, D. J. Twisselmann, and A. Kunz, Phys. Rev. Lett. **90**, 227601 (2003).
[24]P. Pincus, Phys. Rev. **118**, 658 (1960).
[25]Y. V. Khivintsev, L. Reisman, J. Lovejoy, R. Adam, C. M. Schneider, R. E. Camley, and Z. J. Celinski, J. Appl. Phys. **108**, 023907 (2010).
[26]H. Ohldag, A. Scholl, F. Nolting, E. Arenholz, S. Maat, A. T. Young, M. Carey, and J. Stöhr, Phys. Rev. Lett. **91**, 017203 (2003).
[27]S. K. Mishra, F. Radu, S. Valencia, D. Schmitz, E. Schierle, H. A. Dürr, and W. Eberhardt, Phys. Rev. B **81**, 212404 (2010).
[28]M. Ali, C. H. Marrows, M. Al-Jawad, B. J. Hickey, A. Misra, U. Nowak, and K. D. Usadel, Phys. Rev. B **68**, 214420 (2003).
[29]C. Tsang and K. Lee, J. Appl. Phys. **53**, 2605 (1982).
[30]S.-F. Cheng and P. Lubitz, J. Appl. Phys. **87**, 4927 (2000).
[31]A. Ercole, W. S. Lew, G. Lauhoff, E. T. M. Kernohan, J. Lee, and J. A. C. Bland, Phys. Rev. B **62**, 6429 (2000).
[32]H. Xi, R. M. White, and S. M. Rezende, J. Appl. Phys. **87**, 4960 (2000).